Yb, intercalates exhibit gradual coordination transitions with increasing x from 6-fold to 3-fold and from 3-fold to 2-fold, respectively. At low metal concentrations, the complexes are probably discrete units, in which case a mixture of 6- and 3-fold complexes or 3- and 2-fold complexes may coexist in the transition region for the Sr–NH$_3$ and Yb–NH$_3$ compounds, respectively. The complex behavior for Sr may be related to the "softness" of the large Sr^{2+} ion, which results in a poorer definition of its solvation sphere. The rather poor resolution of NH$_3^s$ and NH$_3^w$ for Ba–NH$_3$ compounds supports this view. Such coordination number transitions underscore the delicate balance between the guest–guest and guest–host interactions in these materials.

The Ca and Sr intercalates in this study are stage I, monolayer compounds having a 3R-type structure. The cell constants of the intercalates are in the range a = 3.421 ± 0.003 Å and c = 26.2 ± 0.06 Å over the entire concentration range examined, with no systematic variations. The resulting 3.04 ± 0.02 Å occupied-layer expansion (OLE) is less than previously observed for $(ND_4^+)_{0.22}(ND_3)_{0.34}TiS_2^{0.22-}$,[21] where ammonia is responsible for the observed OLE of 3.21 Å. However, it is significantly greater than the OLE range observed for stage II $(NH_4^+)_{y'}TiS_2^{y'-}$ (2.54–2.85 Å),[22] indicating NH$_3$ is still responsible for the observed OLEs for these intercalates. The independence of the OLE from NH$_4^+$ concentration lends further support to this conclusion. Consequently, these 6-, 3-, and 2-fold solvated complexes are two-dimensional in nature. The observed two-dimensional coordination numbers fit very well with hexagonal host–layer symmetry and trigonal–prismatic guest sites. The XPD intensities are similar to those observed for ammoniated and lithium–ammoniated TiS$_2$ intercalates,[15,21] indicating similar layer structures with trigonal prismatic guest sites for these intercalates. Combined XPD and NPD investigations for selected compounds are in progress.

In summary, we have found that (1) Yb, Ca, Sr, and Ba form two-dimensional solvation complexes with NH$_3$ in TiS$_2$, (2) higher values of metal ion q/r prefer lower coordination numbers, (3) these complexes exhibit coordination number transitions as a function of metal concentration, and (4) the solvation numbers are strongly influenced by the symmetry of the host. The definition of the solvation sphere for Ba^{2+} in these compounds is rather poor, although the presence of NH$_3^s$ could be detected by DSC. Attempts to study the strong complexation expected for Mg–NH$_3$ compounds has not been successful to date due to the low solubility of Mg in NH$_3$. Furthermore, preliminary results indicate that Ca also forms two-dimensional solvation complexes with NH$_3$ between the layers of NbS$_2$, which suggests that the formation of such two-dimensional solvated complexes may indeed be a general phenomenon.

A full account of our work on the existence of metal–ammonia solvation complexes in lamellar transition metal disulfides will be published in the near future.

Acknowledgment. We are grateful to the National Science Foundation for support through Grant DMR-8605937 and the Center for Solid State Science for the use of its Materials Preparation Facility. We also acknowledge the Department of Chemistry for the use of its X-ray Facility and Glass Shop.

---

(21) Young, Jr., V. G.; McKelvy, M. J.; Glaunsinger, W. S.; Von Dreele, R. B. *Solid State Ionics* **1988**, *26*, 47–54.

(22) McKelvy, M. J.; Wiegers, G. A.; Dunn, J. M.; Young, Jr., V. G.; Glaunsinger, W. S. *Solid State Ionics* **1990**, *38*, 163–170.

Nonlinear Optical Characteristics of Novel Inorganic Chromophores Using the Zindo Formalism

David R. Kanis, Mark A. Ratner,* and
Tobin J. Marks*

Department of Chemistry and the
Materials Research Center
Northwestern University, Evanston, Illinois 60208

Michael C. Zerner*

Department of Chemistry and the
Quantum Theory Project
University of Florida, Gainesville, Florida 32611

Received August 29, 1990
Revised Manuscript Received December 3, 1990

The search for molecules possessing large second-order optical nonlinearities (i.e., having large β values) is currently an area of intense activity.[1–6] Once identified, such molecules can be incorporated into macroscopic assemblies to form materials exhibiting very large nonlinear optical (NLO) responses. To date, experimental and theoretical efforts have focused primarily on π-conjugated *organic* chromophores, particularly those with electron-withdrawing and electron-accepting substituents linked through an intervening π-backbone.[1–6] As exploratory synthetic efforts expand to include chromophores containing main-group and transition-metal constituents, the need arises for accurate, computationally efficient, and chemically oriented quantum chemical approaches to describing the nonlinear optical properties of such chromophores.

There are several theoretical approaches for calculating molecular nonlinear optical responses. Computationally intensive methods such as coupled Hartree–Fock,[7] derivative Hartree–Fock,[8] correlated wave[9] ab initio, and finite field[7a,9,10] procedures are currently applicable only to molecules of limited size. More elaborate chromophores are generally treated within a perturbative framework where the electronic states created by the laser field are expressed as a sum over unperturbed excited particle–hole states.[7a,11] Since the NLO expansion coefficients are functions of linear optical properties such as excitation energies and dipole matrix elements, the electronic structure models of choice are spectroscopically based semiempirical algorithms. Indeed, previous sum over states (SOS) studies have employed either a modified all-valence CNDO/S[12–15] or a π-electron PPP (Parr–Par-

---

(1) Khanarian, G., Ed. Nonlinear Optical Properties of Organic Materials. *SPIE Proc.* **1990**, *1147*.

(2) Messier, J., Kajar, F., Prasad, P., Ulrich, D., Eds. *Nonlinear Optical Effects in Organic Polymers*; Kluwer Academic Publishers: Dordrecht, 1989.

(3) Khanarian, G., Ed. Nonlinear Optical Properties of Organic Materials. *SPIE Proc.* **1989**, *971*.

(4) Heeger, A. J., Orenstein, J., Ulrich, D. R., Eds. Nonlinear Optical Properties of Polymers. *Mater. Res. Soc. Symp. Proc.* **1988**, *109*.

(5) Chemla, D. S., Zyss, J., Eds. *Nonlinear Optical Properties of Organic Molecules and Crystals*; Academic Press: New York, 1987; Vols. 1, 2.

(6) Williams, D.. J. *Angew. Chem., Int. Ed. Engl.* **1984**, *23*, 690–703.

(7) (a) Jørgensen, P.; Simons, J. *Second Quantization-Based Methods in Quantum Chemistry*; Academic Press: New York, 1981. (b) Caves, T. C.; Karplus, M. J. *J. Chem. Phys.* **1969**, *50*, 3649–3661.

(8) Dykstra, C. E.; Jasien, P. J. *Chem. Phys. Lett.* **1984**, *109*, 388–393.

(9) Sekino, H.; Bartlett, R. J. *J. Chem. Phys.* **1986**, *85*, 976–989.

(10) (a) Zyss, J.; Berthier, G. *J. Chem. Phys.* **1982**, *77*, 3635–3653. (b) Subbaswamy, K. R.; Mahan, G. D. *J. Chem. Phys.* **1986**, *84*, 3317–3319. (c) Parkinson, W. A.; Zerner, M. C., submitted for publication.

(11) Ward, J. F. *Rev. Mod. Phys.* **1965**, *37*, 1–18.

0897-4756/91/2803-0019$02.50/0

Table I. Calculated and Experimental Optical Spectroscopic, Dipole Moment, and Molecular Hyperpolarizability (10^{-30} cm^5 esu^{-1}; $\hbar\omega$ = 0.65 eV) Data for Conventional Organic Chromophores

	D	A	$\beta_{vec}^{expt\ a}$	β_{vec}^{calcd}	μ^{expt},^{a} D	μ^{calcd}, D	$\lambda_{max}^{expt\ a}$, nm	λ_{max}^{calcd}, nm
								
1	F	H	<0.2	−0.36	1.5	1.9		269
2	NH_2	H	0.55	1.55	1.5	1.3		238
3	H	NO_2	1.9	3.19	4.0	6.3		273
4	NH_2	CN	3.1	3.80	5.0	6.6	270	269
5	OCH_3	NO_2	5.1	6.20	4.6	6.3	302	297
6	NH_2	NO_2	9.2	10.6	6.2	8.1	365	317
7	NMe_2	NO_2	12	15.0	6.4	8.5	376	334
8	NH_2	$C_2(CN)_3$	23	20.5	7.8	7.8	498	501
9	NMe_2	$C_2(CN)_3$	30	31.6	8.0	8.5	516	504
				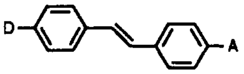				
10	OH	NO_2	17	24.2	5.5	7.1	370	339
11	SCH_3	NO_2	26	25.4	4.3	6.4	374	346
12	OCH_3	NO_2	28	33.2	4.5	7.5	364	363
13	NH_2	NO_2	40	45.7	5.1	9.5	402	376
14	NMe_2	NO_2	83	55.5	6.2	9.9	424	383
				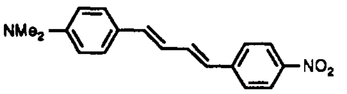				
15			508^b	470^c		11.2	430^b	402

^{a} Data of ref 32. ^{b} Data of ref 35 at $\hbar\omega$ = 1.17 eV. ^{c} Calculated at $\hbar\omega$ = 1.17 eV.

iser–Pople)[16–19] approach to compute frequency-doubling efficiencies. Although these methods have been remarkably successful for predicting and understanding observed nonlinear optical responses, the scope of their application is largely limited to conventional π-organic chromophores. In contrast, the ZINDO (INDO/S, intermediate neglect of differential overlap/spectroscopy) electronic structure formalism has been successfully parametrized for a wide range of main-group and transition-metal elements[20–25] and is therefore potentially ideal for computing the quadratic NLO characteristics of molecules inaccessible to other approximate or semiempirical models. Herein we communicate the first application of ZINDO to calculating the quadratic hyperpolarizabilities of main-group inorganic chromophores.[26] The focus is upon unusual inorganic substituents and conjugation pathways.

Table II. Calculated Optical Spectroscopic, Dipole Moment, and Molecular Quadratic Hyperpolarizability (10^{-30} cm^5 esu^{-1}; $\hbar\omega$ = 0.65 eV) Data for Group-13-Substituted Stilbene Chromophores

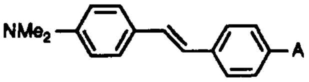

	A	β_{vec}^{calcd}	μ, D	λ_{max}, nm
16	$AlMe_2$	25	2.5	342
17	BF_2	26	5.3	346
18	BH_2	31	4.3	351
19	$AlCl_2$	44	7.8	359
20	BCl_2	45	8.1	365

The fundamental relationship describing the molecular polarization induced by an external electric field can be expressed as a power series:

$$p_i = \sum_j \alpha_{ij}E_j + \sum_{jk} \beta_{ijk}E_jE_k + \sum_{jkl} \gamma_{ijkl}E_jE_kE_l + \ldots \qquad (1)$$

where p_i is the polarization induced along the ith molecular axis, E_j is the applied electric field in the jth direction and α (linear), β (quadratic), and γ (cubic) are the tensor coefficients of the polarization. The formula for the individual components of the quadratic hyperpolarizability responsible for second harmonic generation (SHG) is given from perturbation theory by[11–18]

---

(12) Itoh, Y.; Ohno, K.; Isogai, M.; Kakuta, A. *Mol. Cryst. Liquid Cryst.* **1989**, *170*, 259–272.

(13) Docherty, V. J.; Pugh, D.; Morley, J. O. *J. Chem. Soc., Faraday Trans. 2* **1985**, *81*, 1179–1192.

(14) (a) Lalama, S. L.; Garito, A. F. *Phys. Rev.* **1979**, *A20*, 1179–1194. (b) Garito, A. F.; Teng, C. C.; Wong, K. Y.; Zammani'Khamiri, O. *Mol. Cryst. Liq. Cryst.* **1984**, *106*, 219–258.

(15) Morrell, J. A.; Albrecht, A. C. *Chem. Phys. Lett.* **1979**, *64*, 46–50.

(16) Li, D.; Ratner, M. A.; Marks, T. J. *J. Am. Chem. Soc.* **1988**, *110*, 1707–1715.

(17) Li, D.; Marks, T. J.; Ratner, M. A. *Chem. Phys. Lett.* **1986**, *131*, 370–375.

(18) Dirk, C. W.; Twieg, R. J.; Wagniere, G. J. *J. Am. Chem. Soc.* **1986**, *108*, 5387–5395.

(19) Pople, J. A.; Beveridge, D. L.; Dobosh, P. *J. Chem. Phys.* **1967**, *47*, 2026–2033.

(20) Ridley, J.; Zerner, M. C. *Theor. Chim. Acta (Berlin)* **1973**, *32*, 111–134.

(21) Bacon, A. D.; Zerner, M. C. *Theor. Chim. Acta (Berlin)* **1979**, *53*, 21–54.

(22) Anderson, W. P.; Edwards, W. D.; Zerner, M. C. *Inorg. Chem.* **1986**, *25*, 2728–2732.

(23) Anderson, W. P.; Cundari, T. R.; Drago, R. S.; Zerner, M. C. *Inorg. Chem.* **1990**, *29*, 1–3.

(24) Kotzian, M.; Rösch, N.; Schröder, H.; Zerner, M. C. *J. Am. Chem. Soc.* **1989**, *111*, 7687–7696.

(25) For the application of ZINDO to polarizability (α) calculations, see: (a) Parkinson, W. A.; Zerner, M. C. *J. Chem. Phys.* **1989**, *90*, 5606–5611. (b) Parkinson, W. A.; Zerner, M. C. *Chem. Phys. Lett.* **1987**, *139*, 563–570.

(26) (a) For applications to transition-metal organometallic chromophores, see: Kanis, D. R.; Ratner, M. A.; Marks, T. J. *J. Am. Chem. Soc.* **1990**, *112*, 8203–8204. (b) As an alternative to the direct SOS method, we have also examined the coupled Hartree–Fock (or RPA, random-phase approximation) model and find that the latter does not give as good results for polarizabilities when compared with experiment as does SOS.[10c] There are two potential reasons for this. First, the INDO/S model has been parametrized to molecular electronic spectra at the "monoexcited configuration interaction" (MECI) or "configuration interaction singles" (CIS level), and SOS represents a more consistent application of the model. Second, RPA theory "senses" Hartree–Fock instabilities and can and does lead to spurious results.

$$
\begin{aligned}
\beta_{ijk} + \beta_{ikj} = -\frac{e^3}{4\hbar^2}\Bigg[& \sum_{\substack{n\neq n' \\ n\neq g \\ n'\neq g}} (r^j_{gn'}r^i_{n'n}r^k_{gn} + r^k_{gn'}r^i_{n'n}r^j_{gn}) \times \\
& \left(\frac{1}{(\omega_{n'g} - \omega)(\omega_{ng} + \omega)} + \frac{1}{(\omega_{n'g} + \omega)(\omega_{n}g - \omega)}\right) + \\
& (r^i_{gn'}r^j_{n'n}r^k_{gn} + r^k_{gn'}r^i_{n'n}r^j_{gn})\left(\frac{1}{(\omega_{n'g} + 2\omega)(\omega_{ng} + \omega)} + \right. \\
& \left.\frac{1}{(\omega_{n'g} - 2\omega)(\omega_{ng} - \omega)}\right) + (r^j_{gn'}r^k_{n'n}r^i_{gn} + \\
& r^k_{gn'}r^j_{n'n}r^i_{gn})\left(\frac{1}{(\omega_{n'g} - \omega)(\omega_{ng} - 2\omega)} + \right. \\
& \left.\frac{1}{(\omega_{n'g} + \omega)(\omega_{ng} + 2\omega)}\right) + \\
& 4\sum_n [r^j_{gn}r^k_{gn}\Delta r^i_n({\omega_{ng}}^2 - 4\omega^2) + r^i_{gn}(r^k_{gn}\Delta r^j_n + r^i_{gn}\Delta r^k_n) \times \\
& ({\omega_{ng}}^2 + 2\omega^2)]\frac{1}{({\omega_{ng}}^2 - \omega^2)({\omega_{ng}}^2 - 4\omega^2)}\Bigg] \qquad (2)
\end{aligned}
$$

where ω is the frequency of the applied electric field, $r^i_{mn} = \langle\psi_m|r^i|\psi_n\rangle$ is the matrix element of the displacement operator $r^{(i)}$ along the ith molecular axis between electronic states ψ_m and ψ_n, $\Delta r^i_n = r^i_{nn} - r^i_{gg}$ is the difference between excited-state and ground-state (denoted by g) dipole moments, and $\hbar\omega_{ng}$ is the relative energy separation between the ground state and an excited state ψ_n. For this initial study, the transition-moment matrix elements were computed in dipole length form by using LCAO-MO coefficients and the Pariser approximation[27] for matrix elements over atomic orbitals:

$$r^i_{\kappa\lambda} = \delta_{\kappa\lambda}R^i_\lambda \qquad (3)$$

where R^i_λ is a Cartesian coordinate.

In the present procedure, as in other semiempirical approaches for linear and nonlinear optical properties, the MECI approximation is employed to describe the excited states.[28,29] Ideally, all possible monoexcited states should be included in the summation over ψ_n and ψ_m in eq 2; however, our results indicate that the calculated second-order response converges prior to inclusion of all excited states. For typical molecules, the β_{ijk} components can be calculated to three significant figures by using the 130 ZINDO-derived monoexcited states closest in energy to the ground state and to two significant figures by using only the lowest 60 states. All calibration computations in this work on known chromophores employed the larger CI basis set (molecules **1–15**), while screening computations on new chromophores contained a 60-configuration basis set (molecules **16–30**). Although all 27 components of the β tensor can be computed, only the vector component in the dipolar direction (β_{vec}) is sampled by electric-field-induced second harmonic generation (EFISH) experiments. β_{vec} is given by

$$\beta_{\text{vec}}(-2\omega;\omega,\omega) = \sum_{i=1}^{3}\frac{\mu_i\beta_i}{|\mu|} \qquad (4)$$

where

$$\beta_i = \beta_{iii} + \frac{1}{3}\sum_{j\neq i}(\beta_{jji} + \beta_{jij} + \beta_{ijj}) \qquad (5)$$

The ZINDO semiempirical formalism has been discussed elsewhere.[20–25] This computationally efficient scheme provides an accurate description of linear optical properties for a wide range of molecular structures. Molecular integrals are computed rigorously, neglected, approximated with atomic parameters (ionization potentials, one-center coulomb integrals), or evaluated by using a minimal number of well-defined empirical parameters (one parameter per atom). For the present investigation, the ZINDO algorithm was implemented without any parameter manipulation or basis function alteration. Geometrical parameters employed in this study were taken from standard sources.[30–31]

For initial testing of the ZINDO formalism applied to NLO phenomena, we first compare our theoretical results on known organic chromophores to a recently published, internally consistent set of (experimental) EFISH data.[32] Using results from a single laboratory rather than a compendium of results from several laboratories[33] should minimize deviations due to differing experimental conditions (e.g., differing incident frequencies, solvent polarities, local field models, and data reduction schemes). The experimental β_{vec}, optical spectral, and dipole moment data[32] quoted were measured in nonpolar solvents at λ = 1.91 μm (0.65 eV) and employed an Onsager local field model[34] to calculate the reported molecular quantities. ZINDO-derived and experimental quadratic hyperpolarizabilities for the aforementioned organic chromophores (**1–15**)[32,35] are given in Table I. Note that the calculated β_{vec} values vary over 2 orders of magnitude and are generally in excellent agreement with the experimental measurements. These results persuasively argue that the ZINDO/perturbation theory approach can accurately reproduce EFISH-derived quadratic hyperpolarizabilities determined in nonpolar solvents.

It is next of interest to examine alternatives to NO_2 as electron-acceptor groups. In Table II are shown results for a series of stilbene chromophores in which the NO_2 group in high-β chromophore **13** (Table I) has been replaced by various group-13 Lewis acid/π-acceptor moieties. It can be seen that the substituents expected[36] to have the

---

(27) (a) Pople, J. A. *Trans. Faraday Soc.* **1953**, *49*, 1375–1385. (b) Pariser, R.; Parr, R. G. *J. Chem. Phys.* **1953**, *21*, 466–471.

(28) (a) Linderberg, J.; Öhrn, Y. *Propagators in Quantum Chemistry*; Academic Press: London, 1974. (b) Linderberg, J.; Öhrn, Y. *J. Chem. Phys.* **1967**, *49*, 716–727.

(29) Jorgensen, P.; Linderberg, J. *Int. J. Quantum Chem.* **1970**, *4*, 587–602.

(30) Sutton, L. E., Ed. *Tables of Interatomic Distances and Configuration in Molecules and Ions, Supplement 1956–1959*; The Chemical Society Publication 18; Burlington House: London, 1965.

(31) Bond distance data not available in ref 30 were obtained from: (a) Harshbarger, W.; Lee, G.; Porter, R. F.; Bauer, S. H. *Inorg. Chem.* **1969**, *8*, 1683–1689 (B–N distance). (b) Krebs, B. *Angew. Chem.* **1983**, *95*, 113–134 (B–S distance). (c) Vranks, R. G.; Amma, E. L. *J. Am. Chem. Soc.* **1967**, *89*, 3121–3126 (Al–C distance). (d) Becker, G.; Hartmann, H. M.; Münch, A.; Riffel, H. *Z. Anorg. Allg. Chem.* **1985**, *530*, 29–42 (Si–Li distance). (e) Yannoni, C. S.; Clarke, T. C. *Phys. Rev. Lett.* **1983**, *51*, 1191–1193. (f) Chromophores **23–30** are assumed to have planar, all-trans structures in accord with available structural information (refs 41–44 for polysilanes). (g) Specific parameters used are provided in the supplementary material (see the paragraph at the end of the paper).

(32) Cheng, L.-T.; Tam, W.; Meredith, G. R.; Rikken, G. L. J. A.; Meijer, E. W. In ref 1, pp 61–72.

(33) For a collection of EFISH data from different experimental groups, see: Pugh, D.; Morley, J. O. In ref 5, pp 220–223.

(34) Onsager, L. *J. Am. Chem. Soc.* **1936**, *58*, 1486–1493.

(35) Spangler, C. W.; Hall, T. J.; Saindon, M. L.; Rogers, R. D.; McCoy, R. K.; Birge, R. R.; Fleitz, P. A.; Zhang, C. F. *Proc. IOP Conf.*, July 1989.

(36) Greenwood, N. N.; Earnshaw, A. *Chemistry of the Elements*; Pergamon: Oxford, 1984; pp 220, 268.

Table III. Calculated Optical Spectroscopic, Dipole Moment, and Molecular Quadratic Hyperpolarizability (10^{-30} cm^5 esu^{-1}; $\hbar\omega = 0.65$ eV) Data for Some Inorganic NLO Chromophores

	molecule	β_{vec}^{calcd}	μ, D	λ_{max}, nm
21	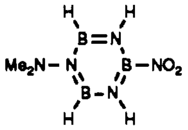	5.4	5.0	341
22	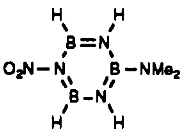	3.2	3.1	319
23	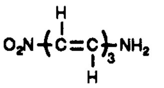 $O_2N\{\overset{H}{C}=\underset{H}{C}\}_3NH_2$	53	12	417
24	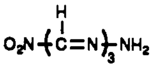 $O_2N\{\overset{H}{C}=N\}_3NH_2$	75	11	471
25	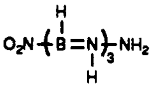 $O_2N\{\overset{H}{B}=\underset{H}{N}\}_3NH_2$	3.5	6.1	232
26	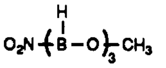 $O_2N\{\overset{H}{B}-O\}_3CH_3$	-0.4	7.4	218
27	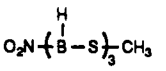 $O_2N\{\overset{H}{B}-S\}_3CH_3$	-1.6	9.1	241
28	$O_2N\{S-S\}_3CH_3$	-1.0	6.0	197
29	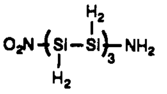 $O_2N\{\overset{H_2}{Si}-\underset{H_2}{Si}\}_3NH_2$	-1.5	5.5	213
30	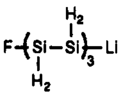 $F\{\overset{H_2}{Si}-\underset{H_2}{Si}\}_3Li$	-10	10	287

greatest Lewis acidity afford predicted β_{vec} values nearly as great as for NO_2.

Inorganic structures offer a variety of novel conjugation pathways, and Table III explores several. The B═N unit forms the basis for numerous π-electron structures with similarities to organic π-systems.[37,38] However, the ZINDO-derived quadratic hyperpolarizabilities for planar borazine chromophores **21** and **22** (Table III) are significantly lower than for the isoelectronic *p*-(dimethylamino)nitrobenzene (**7**). In a comparison of the two borazine derivatives, the larger optical nonlinearity is predicted for **21**, in which the dimethylamino donor group is attached to an electron-rich nitrogen atom and the nitro acceptor group is attached to the electron-deficient boron atom. Our analysis suggests that the β_{vec}-determining transannular charge-transfer excitation in the borazine derivatives is not as strong nor as energetically accessible as the same transition in **7**. Essentially, nitrogen and boron atoms in the heterocyclic ring act as localized donor and acceptor centers, respectively, thus reducing the net electron density redistributed through the ring. In contrast, the β_{vec} values for conventional organic chromophores reflect the ability of an aromatic ring or polyene backbone to act as an effective linkage between electron-rich and electron-deficient groups. In the same vein, calculations on chromophores **23**, **24**, and **25** suggest that the C═N unit can also function as an efficient pathway between donor and acceptor groups, yet the isoelectronic B═N unit again displays poor delocalization characteristics as demonstrated by the predicted β_{vec} and λ_{max} values.

Calculations on chromophores **26**–**30** explore the possibility of using electronically saturated linkages in chromophoric structures. The calculated β_{vec} values and optical absorption wavelengths for molecules **26**–**28** are in accord with the low degree of electron delocalization that such structures exhibit.[39,40] In contrast, saturated polysilanes can exhibit significant degrees of σ-bond electronic delocalization[41-44] and substantial nonresonant *third-order* optical nonlinearities.[45] Since the predominant intramolecular charge-transfer transitions in polysilanes are σ-based rather than π-based, optimal *second-order* nonlinearities should be obtained through σ-donor/σ-acceptor substitution. This is confirmed by the ZINDO-derived β_{vec} values for two all-trans planar polysilanes **29** and **30**, where the computed frequency-doubling efficiency for a polysilane containing π "push–pull" substitution (**29**) is an order of magnitude lower than that of a σ-donor/acceptor polysilane (**30**). Since the predominant $\sigma \rightarrow \sigma^*$ transition in the latter molecule involves charge transfer from a fluorine-based σ-state to a lithium-based σ-state, the direction of the excited-state dipole moment is opposite that of the ground-state dipole moment and a negative quadratic hyperpolarizability is calculated.

In summary, these results indicate that the ZINDO LCAO-SCF formalism can provide an accurate, computationally efficient means of predicting second-order NLO responses for a wide range of unusual organic and inorganic chromophores. The obvious extension of this work to the systematic design of novel chromophores is now in progress.

Acknowledgment. This research was supported by the Air Force Office of Scientific Research (Contracts 86-0105 and 90-0071), by the NSF-MRL program through the Materials Research Center of Northwestern University (Grant DMR882151), and by a grant from the Eastman Kodak Co. We thank Drs. C. S. Willand and W. A. Parkinson for helpful comments and Dr. L.-T. Cheng for generous communication of experimental data.

Supplementary Material Available: Table of metrical parameters employed in the ZINDO calculations (2 pages). Ordering information is given on any current masthead page.

---

(37) Marginggele, W. In *The Chemistry of Inorganic Homo- and Heterocycles*; Haiduc, I., Sowerby, D. B., Eds.; Academic Press: London, 1987; p 17.

(38) Nelson, J. T.; Pietro, W. J. *Inorg. Chem.* **1989**, *28*, 544–548.

(39) Molecule **26** represents linear analogues of B–O heterocycles. See: Haiduc, I. In ref 37, pp 109–141.

(40) Molecule **27** represents linear analogue of B–S heterocycles. See: Siebert, W. In ref 37, pp 143–165.

(41) Miller, R. D. *Angew. Chem., Int. Ed. Engl. Adv. Mater.* **1989**, *28*, 1733–1740.

(42) West, R. J.; Maxka, J. *ACS Symp. Ser.* **1988**, *360*, 6–20.

(43) Miller, R. D.; Rabolt, J. R.; Sooriyakumaram, R.; Fleming, W.; Fickes, G. N.; Farmer, B. L.; Kuzmany, H. *ACS Symp. Ser.* **1988**, *360*, 43–60.

(44) Klingensmith, K. A.; Dawning, J. W.; Miller, R. D.; Michl, J. *J. Am. Chem. Soc.* **1986**, *108*, 7438–7439.

(45) Baumert, J.-C.; Bjorklund, G. C.; Jundt, D. H.; Jurich, M. C.; Looser, H.; Miller, R. D.; Rabaolt, J.; Sooriyakumaran, R.; Swalen, J. D.; Twieg, R. *Appl. Phys. Lett.* **1988**, *53*, 1147–1149.